Targeting QKI-7 in vivo Restores Endothelial Cell Function in Diabetes

Yang et al

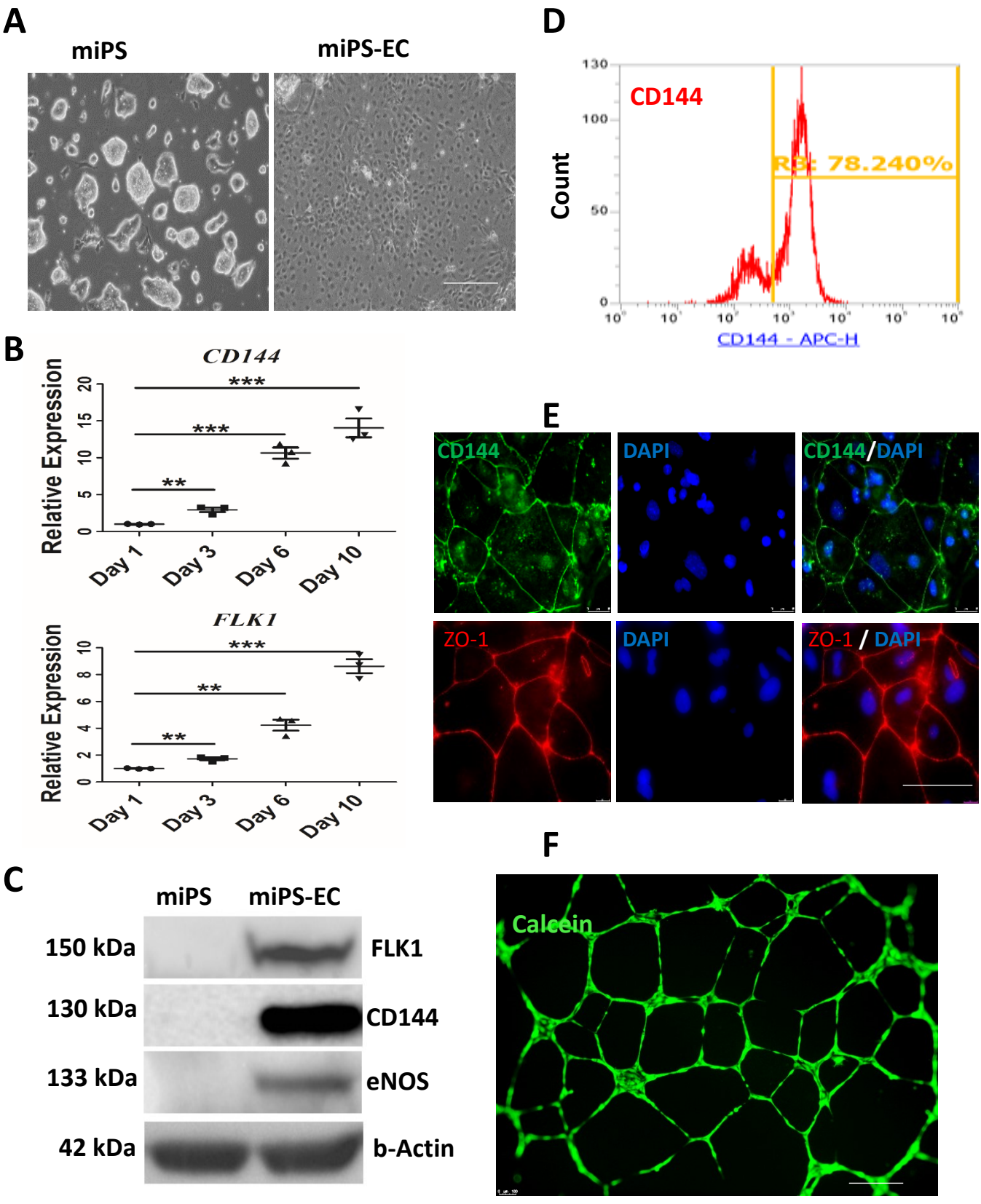

Supplementary Figure 1. Mouse Induced Pluripotent Stem Cells Differentiation towards ECs. Mouse iPS cells were seeded onto plates coated with collagen IV and differentiation media supplemented with 25ng/ml VEGF (DM+V). Morphology of miPSCs and their EC differentiated counterparts are shown by bright field microscopy. Scale bar: 50um (A). The expression level of EC marker genes CD144 (p value: 0.0029, 0.0002, 0.0005) and FLK1 (p value: 0.0026, 0.0014, 0.0001) increased in a time dependent manner during differentiation (B). The expression of EC marker proteins FLK1, CD144 and eNOS is shown by western blot (C). Flow cytometry showed the high efficiency of ECs induction from miPSCs (D). Immunofluorescence confocal image showing that the 6 days differentiated ECs expressed the EC specific markers CD144 and ZO-1 localizing to cell-cell junction. Scale bar: 25μm (E). miPS-ECs formed tube structure indicating their capacity of angiogenesis. Scale bar: 200um (F). Data are from three biologically independent experiments. Error bars represent mean ± SEM (n=3). P values are shown **p < 0.01, ***p<0.001 (two-tailed t test). Source data are provided as a Source Data file.

A

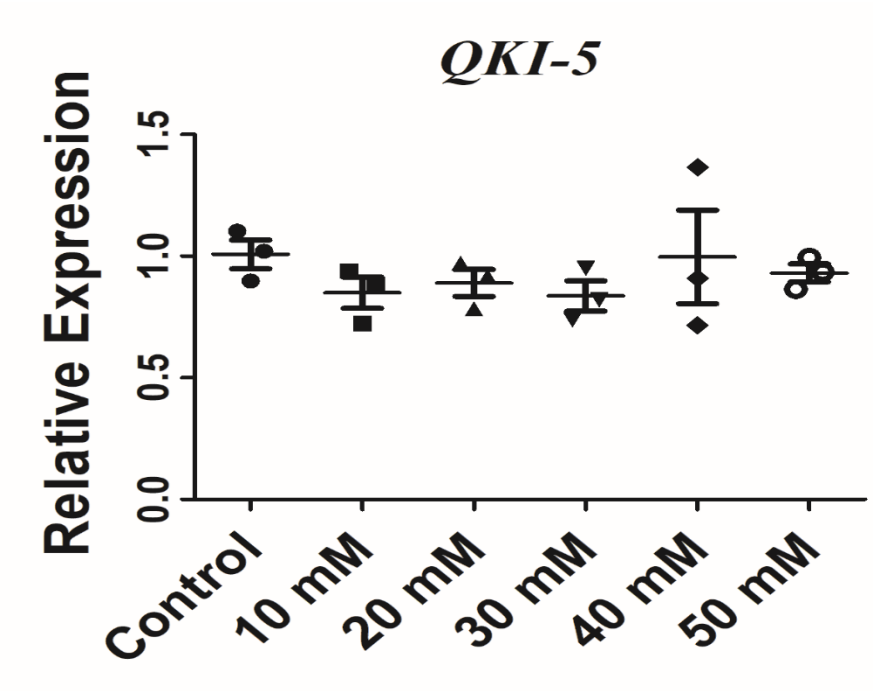

B

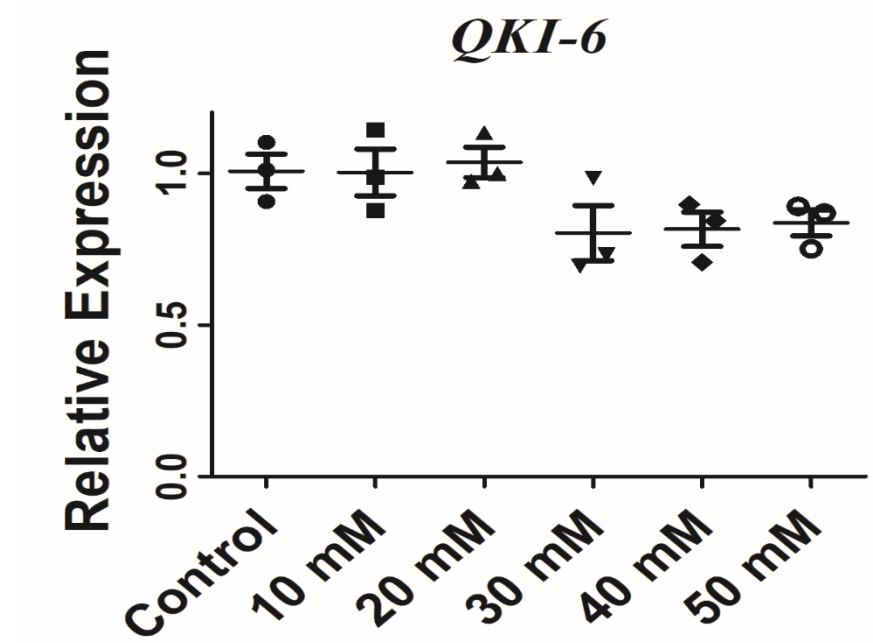

Supplementary Figure 2. QKI-5 and QKI-6 expression levels are not affected by high glucose treatment. (A,B) Upon high glucose treatment of miPS-ECs, QKI-5 and QKI-6 are not effected in mRNA level in dose-dependent experiments. L-glucose treated cells have been used as controls in these experiments. Data are from three biologically independent experiments. Error bars represent mean ± SEM (n=3). Source data are provided as a Source Data file.

A

Results for sequence: sequence1
Genomic position: chr6:163563493-163564892 **Strand:** +
View binding sites predictions summary

Protein: CUG-BP(Hs/Mm)

Position	Genomic coordinate	Motif	Occurrence	Z-score	P-value
106	chr6:163563598	ugcug	ugccaaacggaacuccucacccaacugcugcaauaguuccuccagggcccgaagc	2.221	1.32e-02
1221	chr6:163564713	ugcug	ugccugauauuucagcccauugacugcugcgaugaaggacuagaauacagcagcu	2.257	1.20e-02
1357	chr6:163564849	ugcug	uuuccugaauuguauaugaccuuggugcugcaugcaugcuguugacuuuuaggac	3.496	2.36e-04
1368	chr6:163564860	ugcug	guauaugaccuuggugcugcaugcaugcuguugacuuuuaggacuuugaucuuuu	3.442	2.89e-04

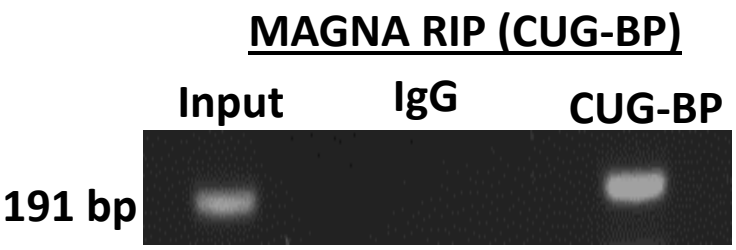

Primer F	TGTGTCACATTACTGGGCAA
Primer R	CACCAGCACCCTTGTATAGTAA

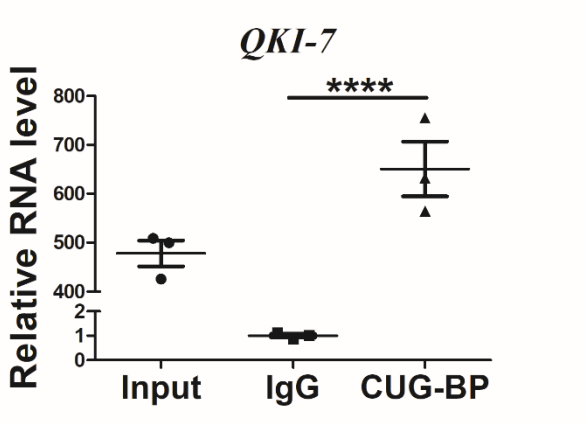

B

Results for sequence: sequence1
Genomic position: chr6:163563493-163564892 **Strand:** +
View binding sites predictions summary

Protein: HNRNPM(Hs/Mm)

Position	Genomic coordinate	Motif	Occurrence	Z-score	P-value
448	chr6:163563940	gguugguu	gauccacuuugguaacugagguucaguuugguugggguaaaucuguuguguacauuuca	4.444	4.42e-06
452	chr6:163563944	gguugguu	cacuuugguaacugagguucaguuugguugggguaaaucuguuguguacauuucaacaa	4.413	5.10e-06

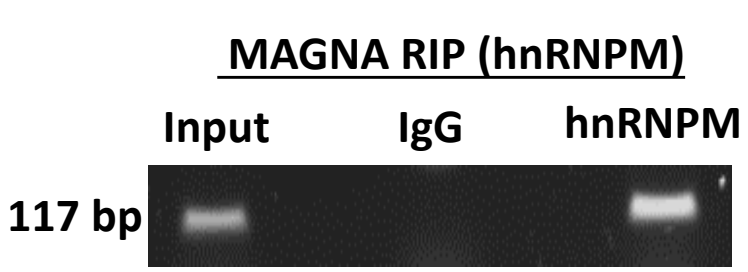

Primer F	TTGCTCACCGGAACCTTAGT
Primer R	AGCCAAACCAAACACACCTT

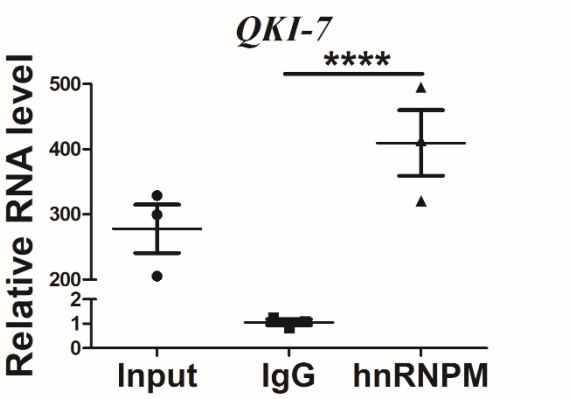

Supplementary Figure 3. Verification of predicted RNA binding sites for CUG-BP and hnRNPM within QKI-7 sequence. (A) Predicted RNA binding motifs of CUG-BP located at the intron 6-exon 7 interface district of QKI-7 gene sequence, and validation based on RNA Immunoprecipitation (RIP) experiments. (B) Predicted RNA binding motifs of hnRNPM located within the intron 6 district of QKI-7 gene sequence, and validation based on RNA Immunoprecipitation (RIP) experiments. Data are from three biologically independent experiments. Error bars represent mean ± SEM (n=3). P values are shown ****<0.0001 (two-tailed t test). Source data are provided as a Source Data file.

A

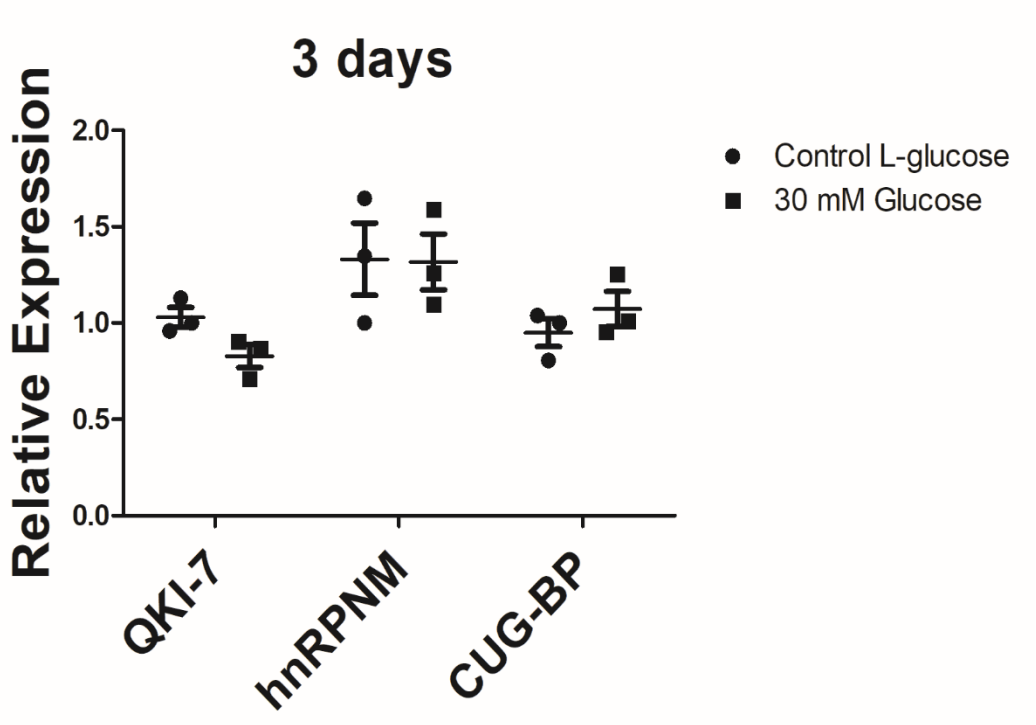

B

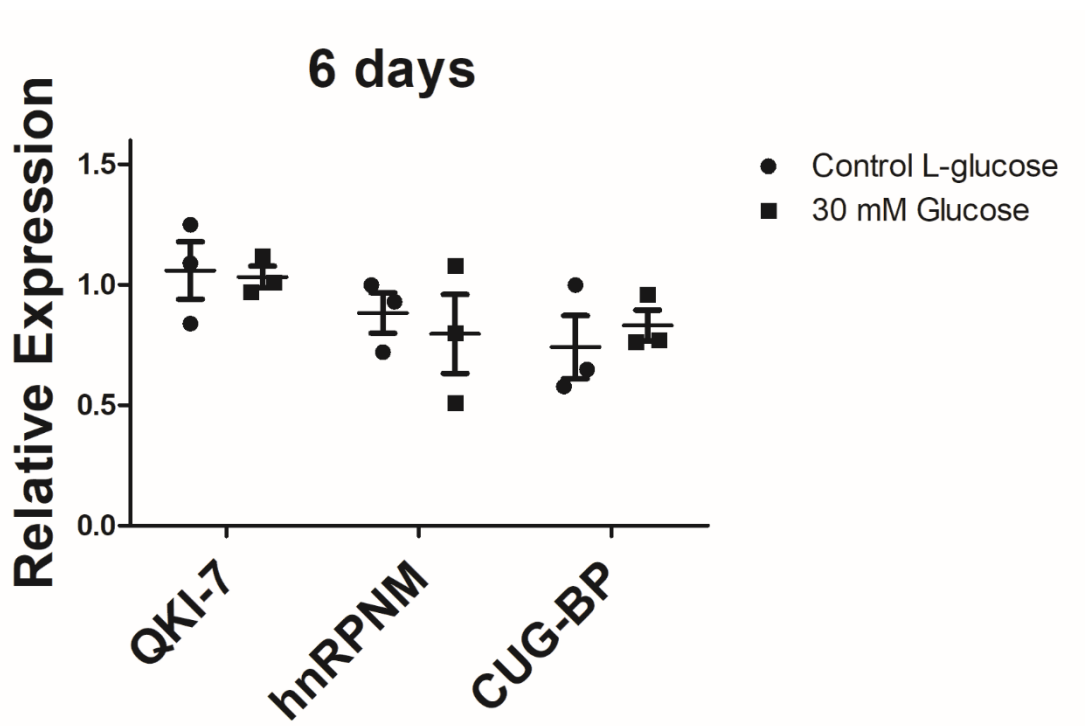

Supplementary Figure 4. Neither the QKI-7 expression levels nor the splicing factors hnRPNM, and CUG-BP altered when human Fibroblasts were treated with high glucose. (A,B) Upon high glucose stimulation of human fibroblasts for 3 **(A)** and 6 days **(B)** the QKI-7, hnRPNM, and CUG-BP expression levels were tested in mRNA levels by real time PCR. L-glucose treated cells have been used as controls in these experiments. Data are from three biologically independent experiments. Error bars represent mean ± SEM (n=3). Source data are provided as a Source Data file.

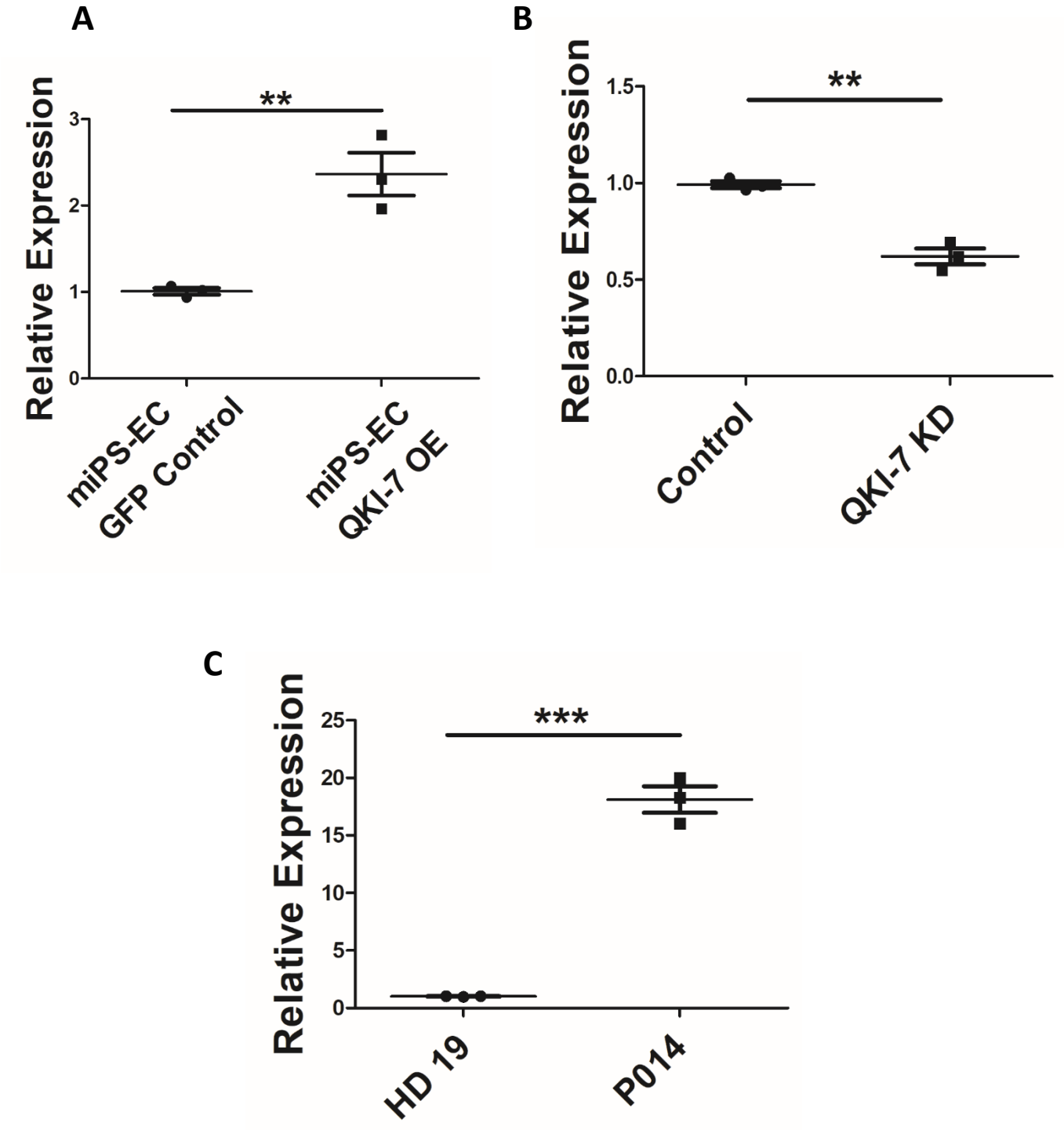

Supplementary Figure 5. QKI-7 regulated IL-1β gene expression. (A) QKI-7 overexpression in miPS-ECs upregulated IL-1β expression. (p value: 0.0053). (B) With QKI-7 knockdown, IL1b expression was downregulated. (p value: 0.0011). (C) Compared to the non-diabetic donor hiPS-ECs HD19, diabetic hiPS-ECs P014 showed higher expression level of IL1b (p value: 0.0001). Data are from three biologically independent experiments. Error bars represent mean ± SEM (n=3). P values are shown **p<0.01, ***p<0.001 (two-tailed t test). Source data are provided as a Source Data file.

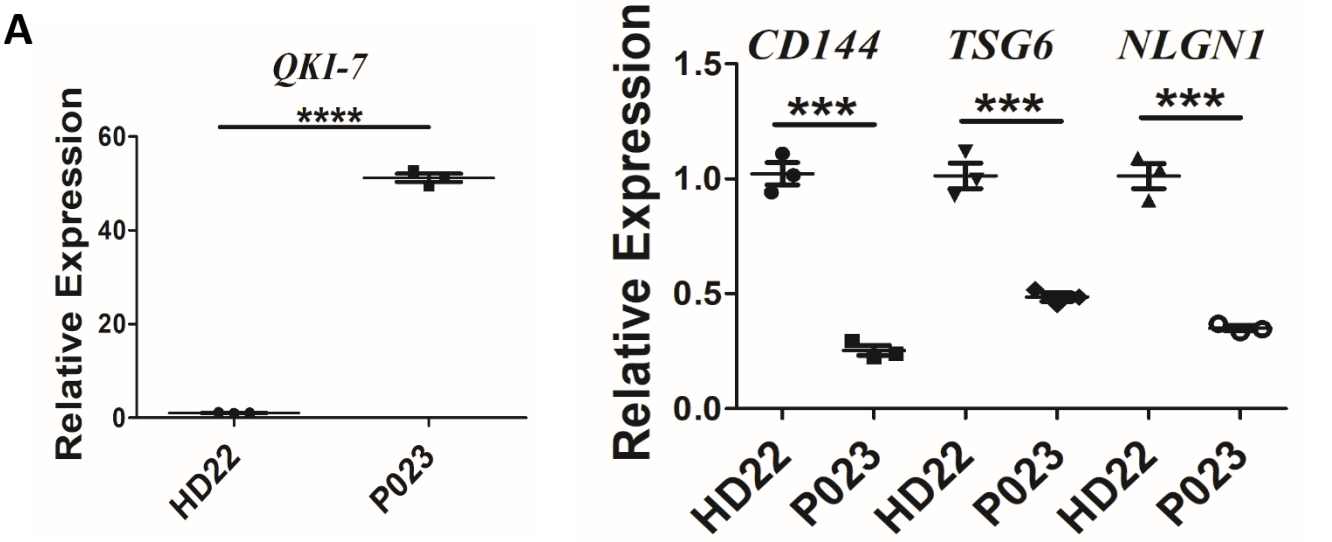
A
QKI-7
****
Relative Expression
60
40
20
0
HD22
P023
CD144
TSG6
NLGN1
***
***
***
Relative Expression
1.5
1.0
0.5
0.0
HD22
P023
HD22
P023
HD22
P023

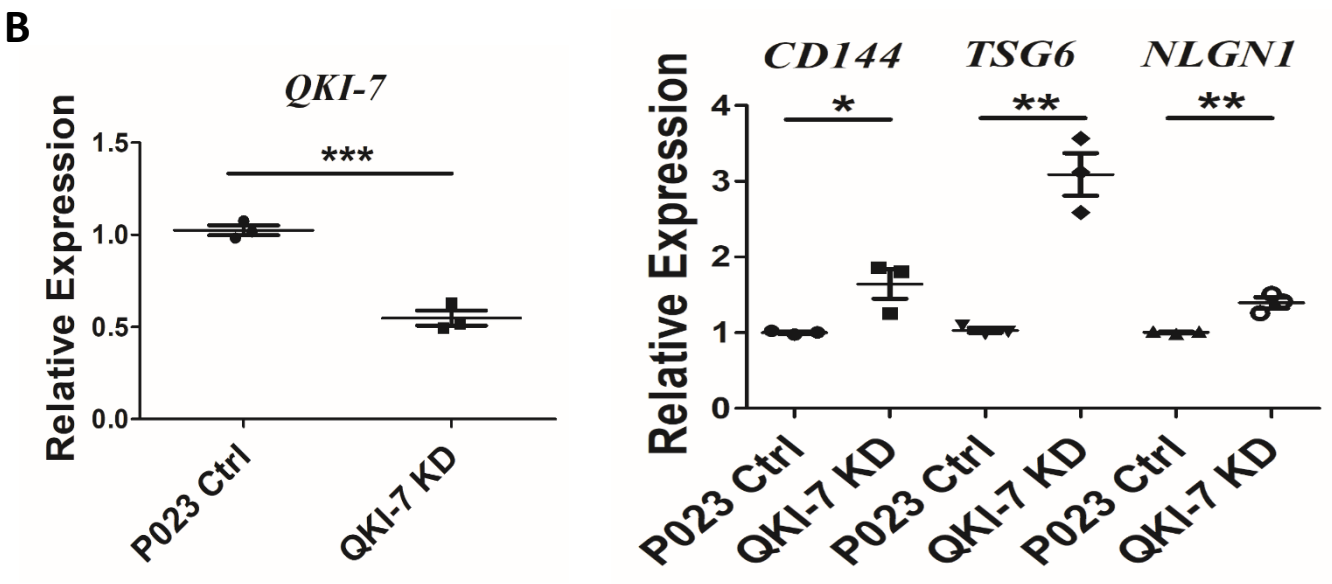
B
QKI-7
***
Relative Expression
1.5
1.0
0.5
0.0
P023 Ctrl
QKI-7 KD
CD144
TSG6
NLGN1
*
**
**
Relative Expression
4
3
2
1
0
P023 Ctrl
QKI-7 KD
P023 Ctrl
QKI-7 KD
P023 Ctrl
QKI-7 KD

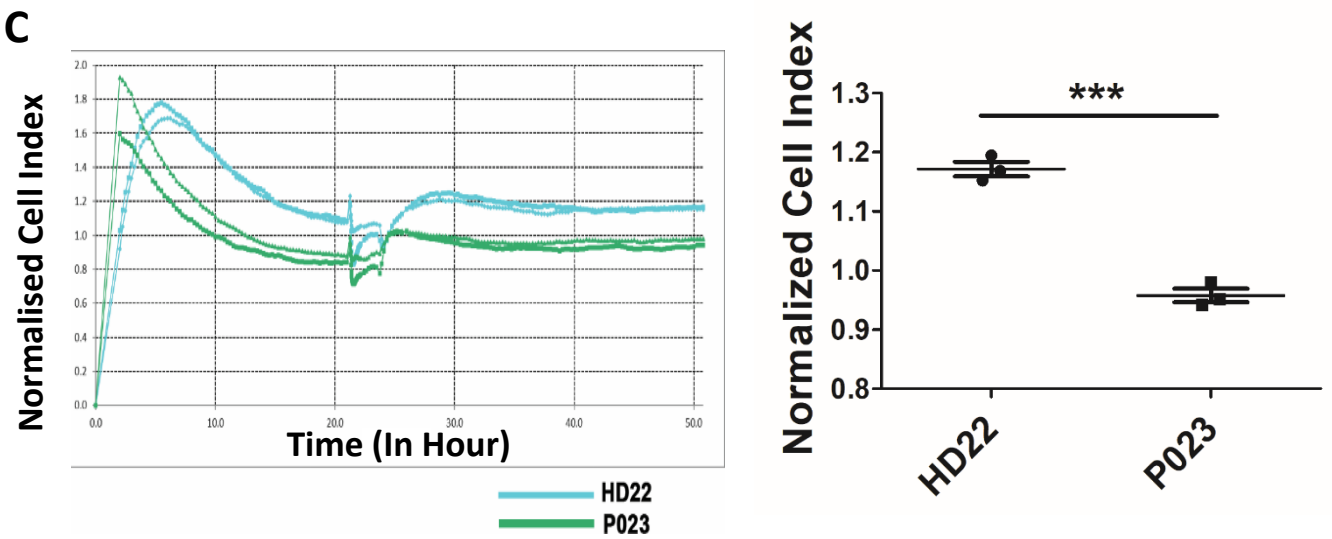
C
Normalised Cell Index
Time (In Hour)
HD22
P023
Normalized Cell Index
***
1.3
1.2
1.1
1.0
0.9
0.8
HD22
P023

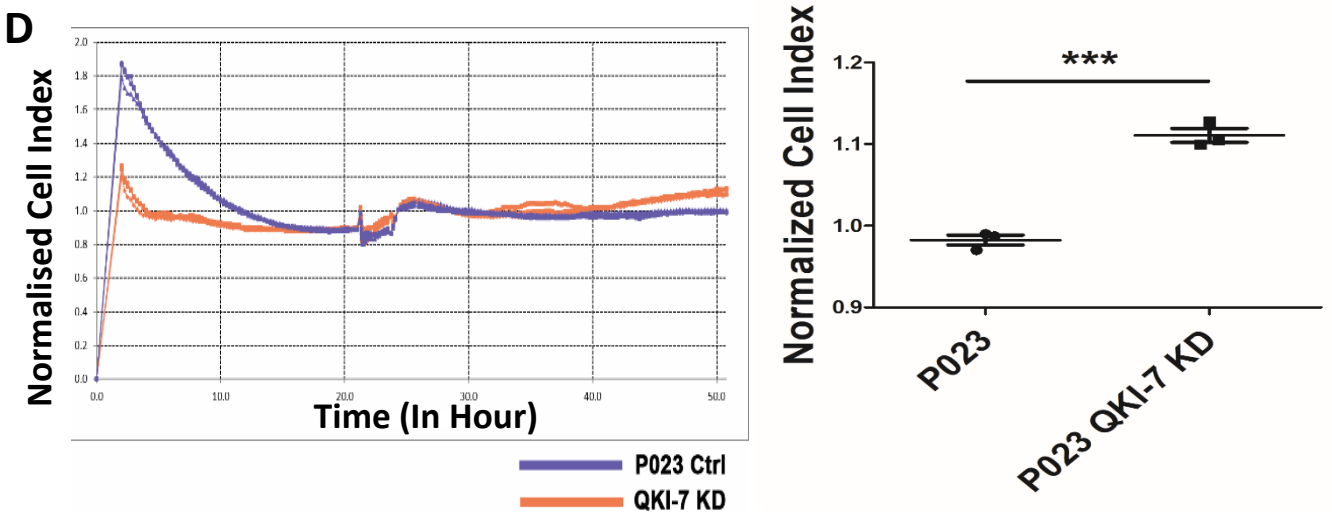
D
Normalised Cell Index
Time (In Hour)
P023 Ctrl
QKI-7 KD
Normalized Cell Index
***
1.2
1.1
1.0
0.9
P023
P023 QKI-7 KD

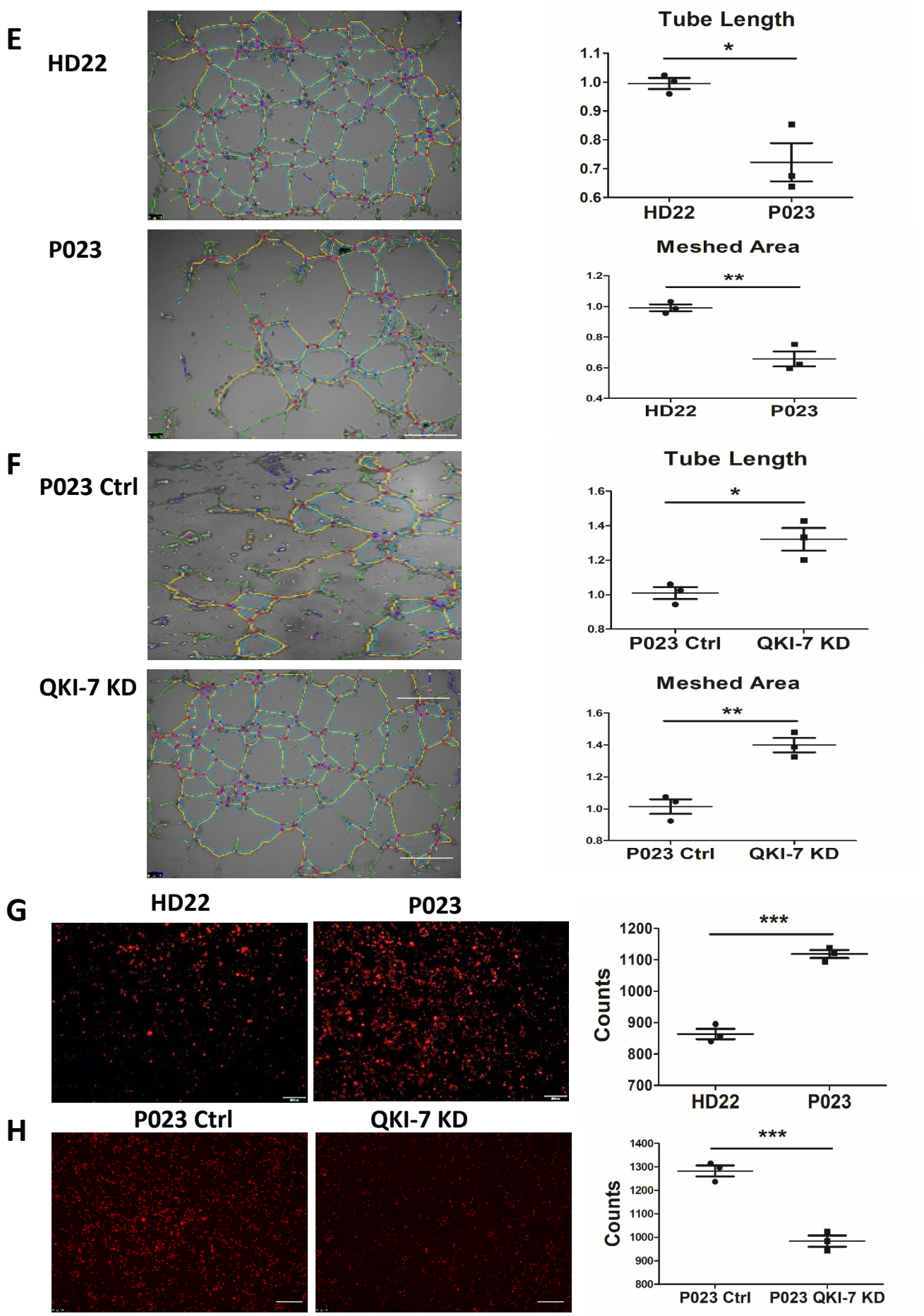

Supplementary Figure 6. QKI-7 regulated expression of CD144, TSG6, NLGN1 and affected endothelial functions of hiPS-ECs. (A) Compared to non-diabetic donor hiPS-ECs HD22, diabetic P023 showed higher QKI-7 expression and lower level of CD144, TSG6 and NLGN1 (p values: <0.0001, 0.0001, 0.0009, 0.0003). (B) With QKI-7 knockdown in diabetic hiPS-ECs P023, CD144, TSG6, NLGN1 expression levels significantly increased (p values: 0.0006, 0.0293, 0.0019, 0.0063). (C) Compared to healthy donor hiPS-ECs HD22, diabetic P023 showed significantly lower RTCA cell index indicating a permeability increase (p value: 0.0002). (D) With QKI-7 knockdown, P023 RTCA cell index was enhanced, showing the alleviation of cell barrier defect (p value: 0.0003). (E) By tube formation assay, diabetic iPS-EC P023 formed less capillary structure than HD22 non-diabetic cells, measured by shorter tube branch length and smaller meshed area (p values: 0.0167, 0.0033). (F) With QKI-7 knockdown, more capillary structure was established in diabetic iPS-EC P023 (p values: 0.0139, 0.0039). (G) Compared to HD22 non-diabetic, the diabetic iPS-EC P023 displayed more THP-1 monocyte adhesion (p value: 0.0002). (H) QKI-7 knockdown suppressed THP-1 monocyte adhesion to diabetic iPS-ECs P023 (p value: 0.0009). Scale bar: E, F 200μm; G, H 100um. Data are from three biologically independent experiments. Error bars represent mean ± SEM (n=3). P values are shown *p<0.05, **p<0.01, ***p<0.001, ****p<0.0001 (two-tailed t test). Source data are provided as a Source Data file.

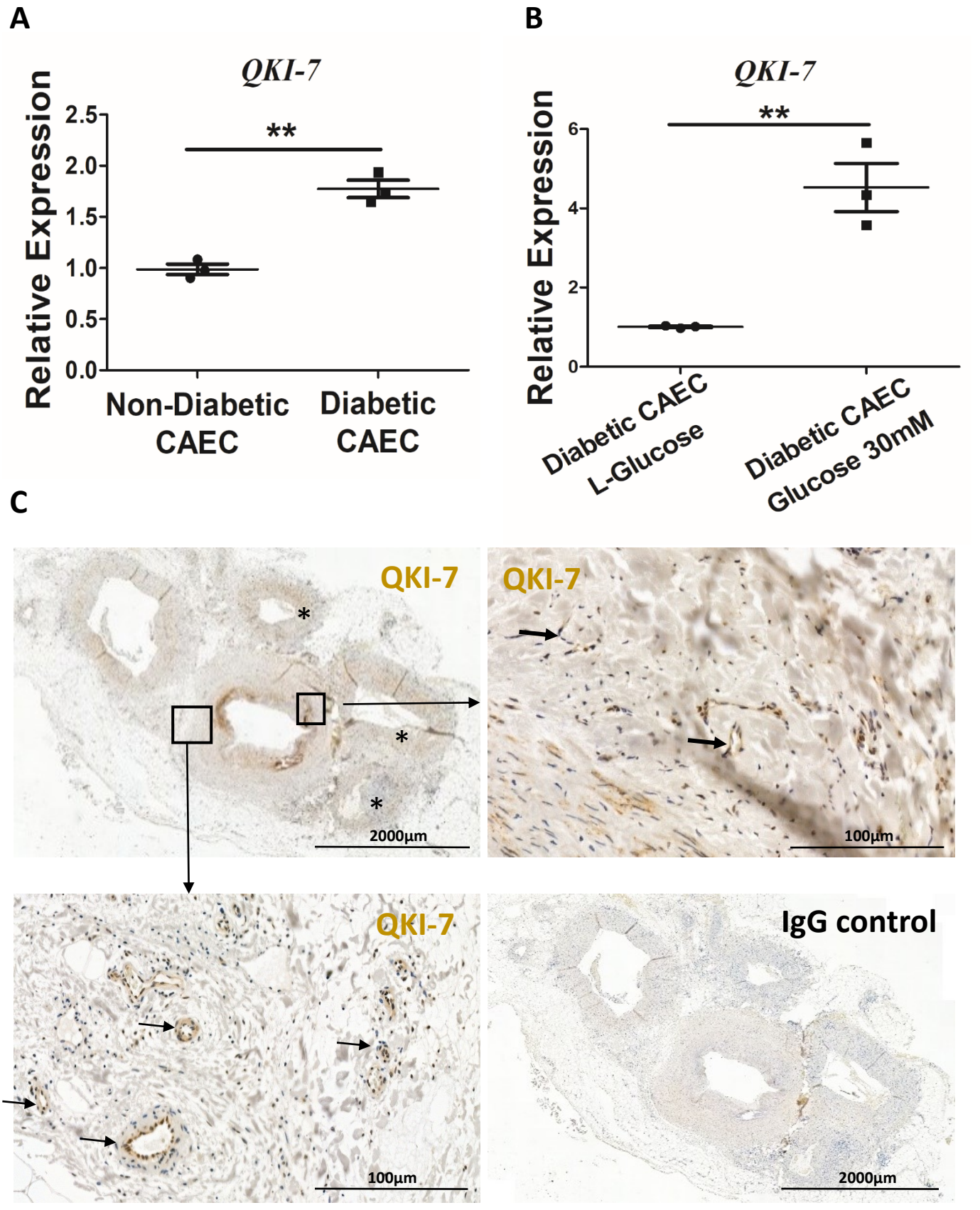

Supplementary Figure S7: QKI-7 is expressed in human Coronary Arterial Endothelial Cells from diabetic donors and in blood vessels of diabetic critical limb ischemia patients. Human Coronary Arterial Endothelial Cells (HCAEC) from non-diabetic and diabetic donors (purchased from Lonza; age, sex, ethnicity matched CC-2585 and CC-2921). (A) QKI-7 high expression was detected in human coronary arterial ECs isolated from diabetic patients, while (p value: 0.0014). (B) QKI-7 was further increased upon 3 days high glucose (30mM) stimulation (p value: 0.0044). Data are from three biologically independent experiments. Error bars represent mean ± SEM (n=3). P values are shown **p<0.01, (two-tailed t test). (C) HRP-DAB immunohistochemical staining on sections of blood vessels obtained from amputated lower limbs of diabetic critical limb ischemia patients was performed detecting QKI-7 expression. Arrows highlight positive endothelial cell staining in microvessels in the adventitia; *staining of endothelium in the vein and smaller artery. IgG control was used as a negative control and sections were counterstained with Mayer's haematoxylin. Scale bars 2000 µm, and 100 µm. Data are from n=3 representative images. Source data are provided as a Source Data file.

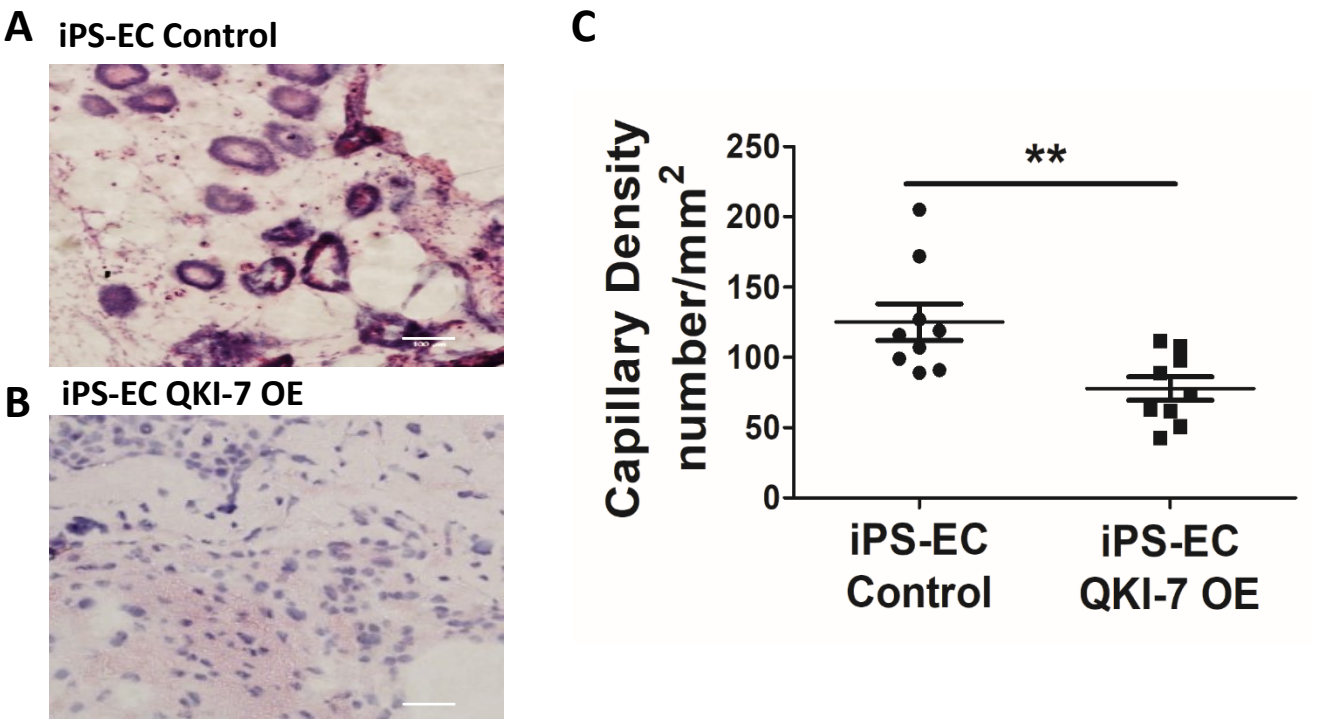

Supplementary Figure 8: QKI-7 overexpression suppressed the in vivo angiogenic capacity of iPS-ECs. Matrigel plug assay was carried out using QKI-7 overexpressing miPS-ECs or control cells (miPS-ECs overexpressing an empty vector). In contrast to the control cells group, QKI-7 overexpression group formed much fewer capillary structures with irregular organization, suggesting an interrupted angiogenetic capacity of ECs (A-C). Images and Quantification from Hematoxylin and Eosin staining. Scale bars: 100um. P value: 0.0076. Data are from n=9 biologically independent experiments. Error bars represent mean ± SEM (n=9) ** $p<0.01$ (two-tailed t test). Source data are provided as a Source Data file.

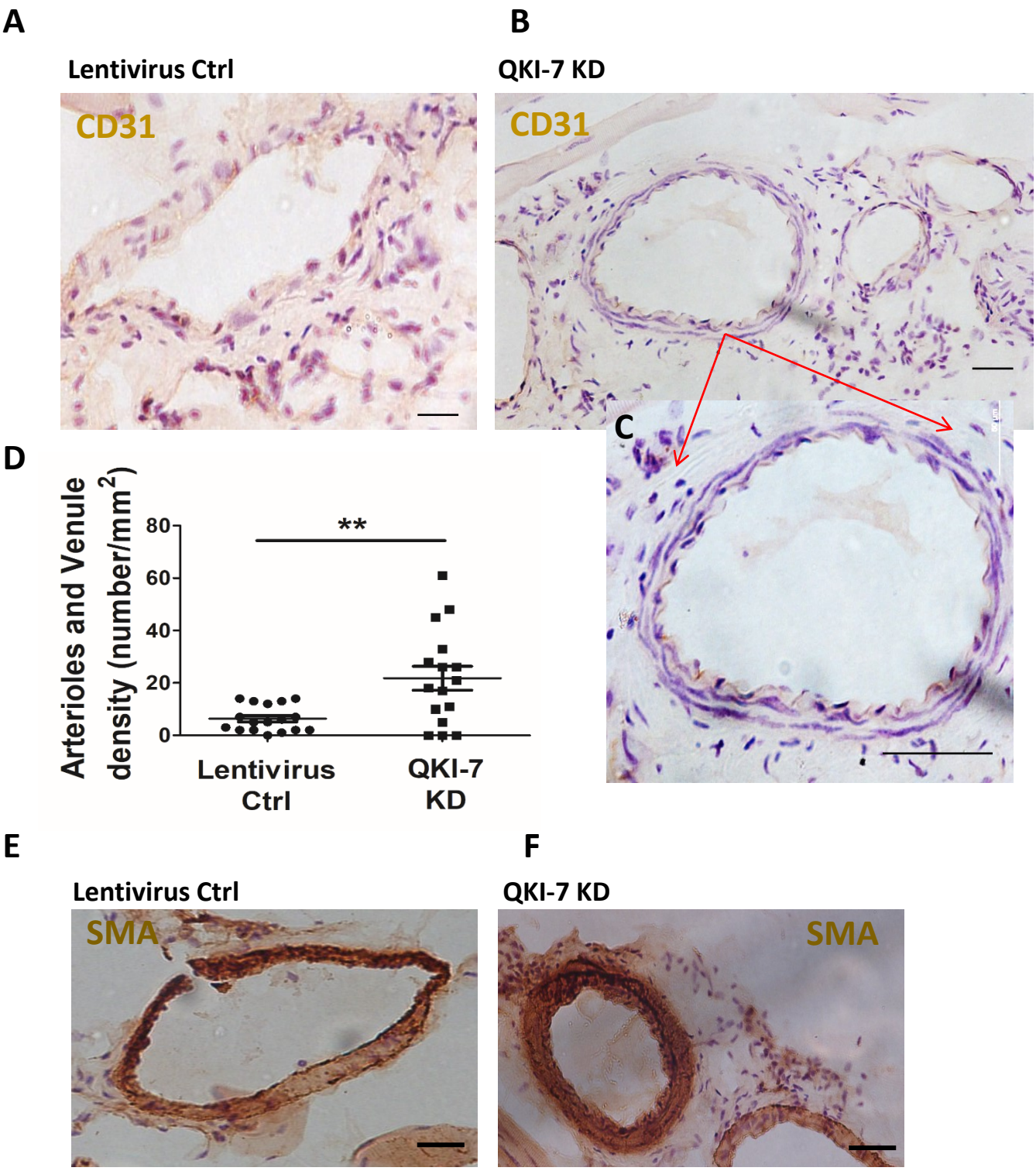

Supplementary Figure 9: Targeting QKI-7 expression in vivo restored EC function in diabetic mice. In vivo QKI-7 knockdown (KD) was achieved by intramuscular injection of shRNA Lentivirus construct tagged with a CD144 promoter and GFP to target ECs, injected in diabetic Hindlimb Ischemic (HLI) skeletal tissue. (A-C) HRP-DAB immunohistochemical staining with CD31 on the sections injected with lentiviral shQKI-7 (KD) showing increased arterioles and venule density. Scale bar: 100 µm and 50 µm in C. Quantification is shown in D (p value: 0.002). Data are from n=16 biologically independent experiments. Error bars represent mean ± SEM (n=16) ** $p<0.01$ (two-tailed t test). (E-F) HRP-DAB immunohistochemical staining for the smooth muscle marker SMA is also shown in E-F, Scale bar: 100 µm. Source data are provided as a Source Data file.

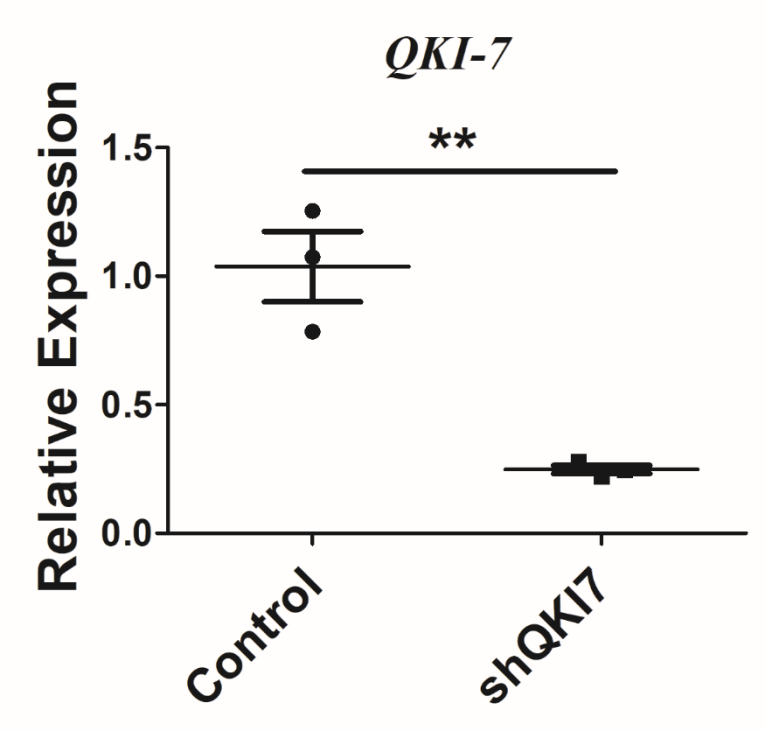

Supplementary Figure 10. Efficiency of pLV[miR30-shRNA]-Cd144>EGFP construct in vitro. The efficiency of the shQKI-7 construct (pLV[miR30-shRNA]-Cd144>EGFP) was tested in vitro when iPS-ECs were infected by lentiviral gene transfer and harvested 72 hours later. The expression levels of QKI-7 were tested in mRNA levels validating the efficient knockdown of QKI-7 in ECs (p value: 0.0046). Data are from three biologically independent experiments. Error bars represent mean ± SEM (n=3). P values are shown **p<0.01 (two-tailed t test). Source data are provided as a Source Data file.

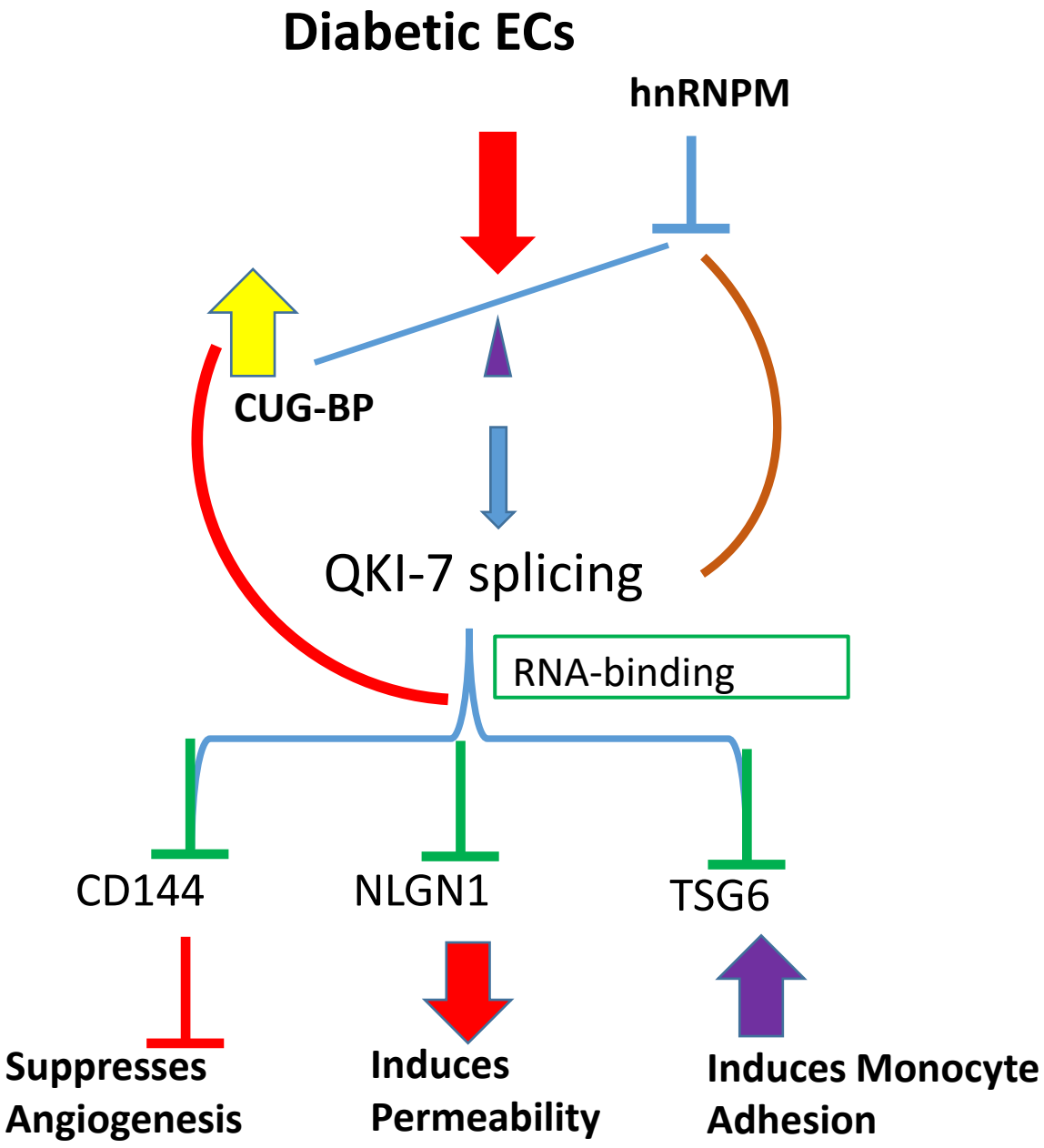

Supplementary Figure 11. Schematic Diagram showing the novel role of QKI-7 in the pathogenesis of diabetes. The imbalance of CUG-BP/hnRNPM regulation in diabetic ECs leads to upregulation of QKI-7, which in turn enhanced the mRNA degradation of RNA-binding targets CD144, TSG6 and NLGN1 and contributed to diabetic endothelial dysfunctions including increased permeability, impaired tube formation and increase of monocyte adhesion.

Supplementary Figure 12 **Yang et al**

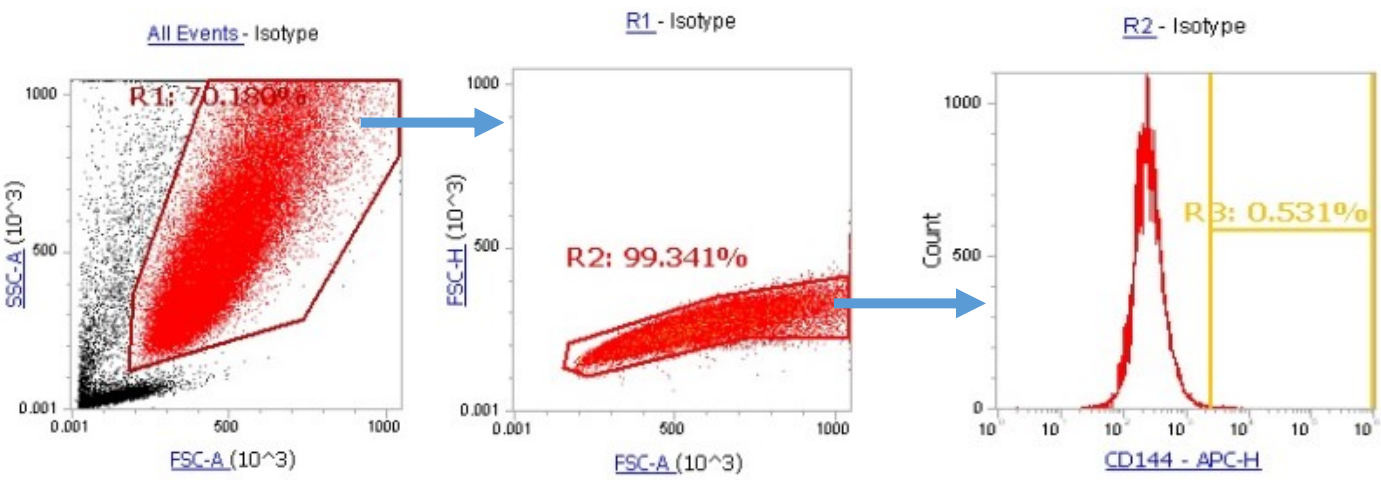

Supplementary Figure 12. Gating strategy to determine the percentage of CD144^{+} hiPS-EC cells after MACS selection in Figure 3B and the percentage of ECs differentiated from miPSCs in supplementary figure 1D.

Gene name	Forward	Reverse
mouse QKI-5	TCCTTGGACCTAGAGGACTTAC	CCGCTCTCTTCAGCTTGATT
mouse QKI-6	ACCCAGTGGTGTGTTAGGTA	GAGGGTTCGGTTAAGACCGT
mouse QKI-7	CCCAGTGGTGTGTTAGAGTGG	ATCCAGCAAGTCAATGGGCTG
mouse CD144	CCACTGCTTTGGGAGCCTT	GGCAGGTAGCATGTTGGGG
mouse eNOS	CTGCCACCTGATCCTAACTTG	CAGCCAAACACCAAAGTCATG
mouse KLF1	ATAGAAGGTGCCCAGGAAAAG	TCTTCAGTTCCCCTTCATTGG
mouse β-Actin	GAGGTATCCTGACCCTGAAGTA	GCTCGAAGTCTAGAGCAACATAG
mouse NLGN1	ACAGTCAACTATCGGCTTGGG	AAACACAGTGATTCGCAAGGG
mouse TSG6	GGGATTCAAGAACGGGATCTTT	TCAAATTCACATACGGCCTTGG
mouse CUGBP	CAGAGGTTGTGCATTTGTGAC	TCTGTTCTTTGTCCTTCTGGG
mouse HNRNPM	CCCAAATGAGATTATCCATGC	TCCAGCCAACTTTATAATCCAGA
mouse IL1b	AGTTGACGGACCCCAAAAG	AGCTGGATGCTCTCATCAGG
human QKI-5	CTCTTGCAGCAACAGCCCAGGC	TTAGTTGCCGGTGGCGGCTCGG
human QKI-6	CTCTTGCAGCAACAGCCCAGGC	TTAGCCTTTCGTTGGGAAAGCC
human QKI-7	CTCTTGCAGCAACAGCCCAGGC	TCAATGGGCTGAAATATCAGGC
human CD144	AAACACCTCACTTCCCCATC	ACCTTGCCCACATATTCTCC
human eNOS	GGTACATGAGCACTGAGATCG	GCCACGTTGATTTCCACTG
human KDR	ATAGAAGGTGCCCAGGAAAAG	GTCTTCAGTTCCCCTCCATTG
human GAPDH	CATGTTCGTCATGGGTGTGAACCA	ATGGCATGGACTGTGGTCATGAGT
human NLGN1	ATGATGGAAGTGTCTTGGCAAGTT	CTTTGCAGCCTGATCGCCTGTA
human TSG6	TCACCTACGCAGAAGCTAAGGC	TCCAACTCTGCCCTTAGCCATC
human IL1b	CCACAGACCTTCCAGGAGAATG	GTGCAGTTCAGTGATCGTACAGG

Supplementary Table 1. List of Primers